

Magnetoconductivity and Polar Scattering in Moderately Ionic Crystals*

F. GARCIA-MOLINER†

Physics Department, University of Illinois, Urbana, Illinois

(Received 24 January 1963)

The dc transport problem in a polar crystal, in the range of optical mode scattering, is studied within a weak-coupling model for the electron-phonon interaction. A full variational calculation is performed in the presence of a magnetic field and carried out to high accuracy on a digital computer. It is stressed that the physical effects should be discussed in "magnetoconductivity," rather than conventional "magnetoconductivity" terms, corresponding to the type of experimental arrangement frequently used for these materials. The model, which is, in principle, restricted to a small coupling constant ($\alpha \ll 1$), has some interesting dispersive properties and is used as a working tool for an over-all picture of the transport problem in its full complexity, when a magnetic field is present. Some experimental aspects are discussed and it is suggested that a heuristic correction to the weak-coupling formulas might extend its practical range of applicability to higher values of α . This is illustrated with applications to AgBr and AgCl, where $\alpha \approx 2$.

I. INTRODUCTION

IN an ionic crystal the conduction electrons interact rather strongly with the longitudinal polarization waves due to optical mode vibrations of the lattice. The strength of this interaction can be measured¹ by a dimensionless coupling constant $\alpha = (m/2\omega\hbar^2)^{1/2} \times e^2(\epsilon_\infty^{-1} - \epsilon_s^{-1})$, where ϵ_s is the static dielectric constant of the crystal, ϵ_∞ is the high frequency dielectric constant, ω is the frequency of the longitudinal optical modes, and m is the crystal band mass (here distinguished from the free electron mass m_e).

In the weak-coupling limit, $\alpha \ll 1$, the picture which emerges from standard first-order perturbation theory describes the drift mobility of the charge carriers as limited by first-order scattering processes in which a polar phonon is absorbed or emitted. At low temperatures the carriers undergo, thereby, highly inelastic scattering events. Howarth and Sondheimer² argued that, under such conditions, it is not clear how to describe the scattering in terms of a relaxation time. Instead, they formally solved the Boltzmann equation by a variational procedure. The essential result of their calculation is a numerical function $G(z)$ of the dimensionless variable $z = \hbar\omega/KT = \Theta/T$. From this function one can calculate the conductivity (or the mobility) if one knows the appropriate parameters of the material (dielectric constants, etc.). Howarth and Sondheimer actually used the result of an earlier derivation^{3,4} of the matrix element for the scattering which neglected the contribution of the ion core electrons to the high frequency dielectric constant. This does not affect the function $G(z)$ and is easily corrected; it is automatically

taken into account, for example, if one uses Fröhlich's Hamiltonian.

The Howarth-Sondheimer model for the transport problem, which is, in principle, restricted to $\alpha \ll 1$, has been very useful in many practical cases, as is illustrated by Ehrenreich's extensive work,⁵ among others. Ehrenreich has extended the calculations to the type of isotropic but nonparabolic bands of the III-V compounds and has also included free carrier screening effects. This paper will not be concerned with either these or the recent extension⁶ to a many-ellipsoidal band structure.

The present work is an attempt to study in detail the properties of the weak-coupling model for the dc transport problem in a polar crystal, without additional complications concerning band structure, etc. Motivated by current experimental work at the University of Illinois, it was felt that further study was necessary on certain questions connected with the weak-coupling model.

The first question concerns the limits of practical applicability of the model, i.e., whether some correction may be devised which makes it work up to higher values of α . The variational calculation of the dc mobility is outlined in Sec. II, where the notation is established for the extensions to follow. A heuristic correction is introduced in the mobility formula, and this is then compared with experimental results for AgBr and AgCl where $\alpha = 2$.

The second question concerns the relationship of the model to others in which polar scattering is described in terms of a constant relaxation time. At low temperatures it may be argued¹ that a slow carrier, having absorbed a phonon of very large energy, has a very high probability of immediately re-emitting it. This is the idea of resonant scattering⁷ in which absorption and

* Work supported in part by the Air Force Office of Scientific Research.

† On leave of absence from the Instituto de Fisica "A. Santa Cruz," C.S.I.C., Serrano 119, Madrid, Spain.

¹ H. Fröhlich, *Advan. Phys.* **3**, 325 (1954).

² D. J. Howarth and E. H. Sondheimer, *Proc. Roy. Soc. (London)* **A219**, 53 (1953).

³ H. Fröhlich, *Proc. Roy. Soc. (London)* **A160**, 280 (1937).

⁴ H. Fröhlich and N. F. Mott, *Proc. Roy. Soc. (London)* **A171**, 496 (1939).

⁵ H. Ehrenreich, *J. Phys. Chem. Solids* **2**, 131 (1957); **8**, 130 (1959); *J. Appl. Phys. Suppl.* **32**, 2155 (1961).

⁶ D. J. Olechna and H. Ehrenreich, *J. Phys. Chem. Solids* **23**, 1513 (1962).

⁷ T. D. Schultz, *Phys. Rev.* **116**, 526 (1960); Technical Report No. 9, 1956, MIT Solid State and Molecular Theory Group (unpublished).

emission merge into one second-order process. The calculation for this type of elastic scattering yields a constant relaxation time independent of the kinetic energy of the carrier. With a single isotropic mass, there is then no dispersive behavior in the gas of carriers.

Now, a magnetic field is a probe which can feel the difference between a dispersive and a nondispersive gas. With a single isotropic mass and a constant relaxation time, the resistivity is not changed by a magnetic field, whereas a nonzero magnetoresistivity is exhibited by the (dispersive) model of first-order inelastic scattering, as was pointed out by Lewis and Sondheimer.⁸ A simple observation of magnetoresistivity would seem a decisive experiment. However, in many polar materials this experiment is very hard to perform. In order to measure resistivity, as is usually done in a reasonably good conductor, one has to maintain a measurable steady current through the sample. Rather, the experimental arrangement which seems to be more convenient in these materials consists in maintaining an electric field inside the sample, and then measuring the (transient) drift of charge. Thus, the ordinary concept of magnetoresistivity is irrelevant to the transport coefficient actually measured in these conditions. As a matter of fact, both the dispersive and the nondispersive model exhibit a nonzero magnetoconductivity. These concepts, and other phenomenological relationships, are explained in Sec. III.

One purpose of this work was to take a broader view and formulate the galvanomagnetic properties of the weak-coupling model in "magnetoconductivity language." It is suggested that this should be the policy of future theories which might truly describe polarons (rather than weakly perturbed electrons), since this is likely to be the frame of the experimental information. Thus, for example, Tippins' recent work,⁹ which has elucidated the shape of the conduction band structure in AgBr, and in AgCl, is all magnetoconductivity work (although the measurements were performed at very low temperatures, where optical mode scattering is frozen out).

The variational calculation outlined in Sec. II is extended in Sec. IV where detailed computations of the galvanomagnetic coefficients are performed. The implications of these calculations are discussed in Secs. IV and V, where some suggestions are made for future experimental work.

To sum up, this is the study of the properties of a model. It is simple and not at all rigorous, but it has the practical advantage that the calculations *can* be performed at arbitrary temperatures and magnetic fields. It can be used for an over-all picture of the dc transport problem in its full complexity. It was thought that such a study might be a helpful guide for future developments.

⁸ B. F. Lewis and E. H. Sondheimer, Proc. Roy. Soc. (London) **A227**, 241 (1954).

⁹ H. H. Tippins and F. C. Brown, Phys. Rev. **129**, 2554 (1963).

II. MOBILITY CALCULATION IN A DC ELECTRIC FIELD

Howarth and Sondheimer's calculation is repeated by Ziman¹⁰ in a more concise fashion, in which some irrelevant details of the collision term are omitted by applying the variational method to the original form of the Boltzmann equation. This technique will be adopted here and the theory extended to the case of a magnetic field. Ziman's derivation of the mobility will be now outlined for the sake of establishing the notation.

For a gas of carriers of wave vector \mathbf{k} and kinetic energy $E = \hbar^2 k^2 / 2m$, the nonequilibrium distribution function is written as

$$f_{\mathbf{k}} = f_{\mathbf{k}}^0 - \Phi_{\mathbf{k}} \frac{\partial f_{\mathbf{k}}^0}{\partial E}, \quad (1)$$

where $f_{\mathbf{k}}^0 = A e^{-E/KT}$ is the equilibrium distribution. The basic quantity in this calculation is a quadratic form of the collision operator \hat{P} , which represents the rate of entropy production due to collisions:

$$\begin{aligned} \langle \Phi_{\mathbf{k}} | \hat{P} \Phi_{\mathbf{k}} \rangle &\equiv \int \Phi_{\mathbf{k}} \hat{P} \Phi_{\mathbf{k}} d\mathbf{k} \\ &= \frac{4\pi e^2 \mathfrak{N} m}{\hbar^2 \gamma \omega K T^2} \int \int \{\Phi_{\mathbf{k}} - \Phi_{\mathbf{k}+\mathbf{q}}\}^2 f_{\mathbf{k}}^0 \frac{1}{qk} d\mathbf{k} d\mathbf{q}. \end{aligned} \quad (2)$$

Here \mathbf{q} is the phonon wave vector, \mathfrak{N} is the Bose-Einstein distribution function $[\exp(-\Theta/T) - 1]^{-1}$, and γ^{-1} , which is proportional to the dimensionless constant α , is defined so that it involves no mass parameter:

$$\frac{1}{\gamma} = \frac{\omega^2}{4\pi} \left(\frac{1}{\epsilon_{\infty}} - \frac{1}{\epsilon_s} \right). \quad (3)$$

Changing to an integration over energy, the weighted volume element $d\mathbf{k}$ becomes

$$d\mathbf{k} = \frac{1}{2\pi^2} \left(\frac{2m}{\hbar^2} \right)^{3/2} E^{1/2} dE.$$

With an electric field $\boldsymbol{\mathcal{E}}$ of magnitude \mathcal{E} and unit direction \mathbf{u} , the appropriate form of $\Phi_{\mathbf{k}}$ is $\mathbf{u} \cdot \mathbf{k} \varphi$, where φ is linear in $\boldsymbol{\mathcal{E}}$ and is evaluated to successive orders of approximation with the variational technique. One expands φ and writes, in the n th order of approximation

$$\Phi_{\mathbf{k}}^{(N)} = \mathbf{k} \cdot \mathbf{u} \varphi^{(N)} = \sum_{r=0}^N c_r \varphi_r(\mathbf{k}). \quad (4)$$

In this case the functions used were

$$\varphi_r = \mathbf{k} \cdot \mathbf{u} E^r \quad (5)$$

corresponding to a power series expansion of φ . Equa-

¹⁰ J. M. Ziman, *Electrons and Phonons* (Clarendon Press, Oxford, 1962), Chap. 10.

tions (2) and (4) give

$$\begin{aligned} \langle \Phi_{\mathbf{k}}^{(N)} | P \Phi_{\mathbf{k}}^{(N)} \rangle &= \sum_{r, s=0}^N c_r \langle \varphi_r | P \varphi_s \rangle c_s \\ &\equiv \sum_{r, s=0}^N c_r P_{rs} c_s. \end{aligned} \quad (6)$$

In terms of the dimensionless integrals δ_{rs} of Howarth and Sondheimer (not to be confused with Kronecker's symbol), the result is, after some mathematical manipulations,

$$P_{rs} = \frac{2^3 m^3 e^2 \mathcal{U} A e^{1/2z}}{3\pi \hbar^5 \gamma} (KT)^{r+s} \delta_{rs} \equiv \mathcal{P} (KT)^{r+s} \delta_{rs}. \quad (7)$$

The power dissipated in the collisions is supplied by the external field. From the drift term of the Boltzmann equation one obtains the rate of energy input through an integral of the form

$$\left\langle -e \frac{\partial f_k^0}{\partial E} \mathbf{v} \cdot \mathbf{u} | \Phi_{\mathbf{k}} \right\rangle.$$

Thus, when $\Phi_{\mathbf{k}}$ is expanded as in Eq. (4), one has to evaluate the integrals

$$\mathbf{J}_r = - \int e \mathbf{v} \varphi_r \frac{\partial f_k^0}{\partial E} d\mathbf{k}.$$

Application of the variational principle then says that the unknown coefficients of $\Phi_{\mathbf{k}}^{(N)}$ are obtained from the variational equations

$$\sum_{s=0}^N P_{rs} c_s = \mathbf{J}_r \cdot \mathbf{u} \mathcal{E}. \quad (8)$$

The implication of this is that the total current \mathbf{J} is, in the N th approximation,

$$\mathbf{J} = \sum_{r, s=0}^N \mathbf{J}_r P_{rs}^{-1} \mathbf{J}_s \cdot \mathbf{u}. \quad (9)$$

The matrix terms P_{rs} are given in Eq. (7). Defining

$$F^{(2)} = \frac{\left(z^6 + \frac{37}{4} z^4 + \frac{165}{4} z^2 + \frac{217}{8} \right) K_1^2 - \left(2z^5 + \frac{19}{4} z^3 + \frac{1081}{32} z \right) K_1 K_0 - \left(z^6 + \frac{23}{4} z^4 + \frac{299}{8} z^2 \right) K_0^2}{\left(-\frac{35}{4} z^4 + \frac{75}{2} z^2 + 24 \right) K_1^3 + \left(\frac{3}{2} z^5 + \frac{85}{8} z^3 - 18z \right) K_1^2 K_0 - \left(\frac{47}{4} z^4 + \frac{117}{2} z^2 \right) K_1 K_0^2 - \left(\frac{3}{2} z^5 + \frac{183}{8} z^3 \right) K_0^3}.$$

The Bessel functions K_n are here to be understood as $K_n(\frac{1}{2}z)$. One can now study the limits of high and low temperatures.

The high-temperature limit ($z \ll 1$) is of academic interest only since it might mean actual temperatures of more than 1000°K. However, it is of some interest

$\lambda_r \equiv \Gamma(r+5/2)/\Gamma(5/2)$, evaluation of the integrals \mathbf{J}_r gives

$$\mathbf{J}_r \cdot \mathbf{u} = \frac{e A m^{3/2} (KT)^{3/2}}{2^{1/2} \pi^{3/2} \hbar^4} (KT)^r \lambda_r \equiv \mathcal{J} (KT)^r \lambda_r. \quad (10)$$

The drift mobility (see Sec. III) is

$$\mu = (1/ne) \mathbf{u} \cdot \mathbf{J} \mathcal{E}^{-1}, \quad (11)$$

where n is the carrier concentration. From Eqs. (8) to (11), one can write for the mobility calculated to N th order:

$$\begin{aligned} \mu^{(N)} &= \frac{1}{ne} \sum_{r, s=0}^N (\mathbf{J}_r \cdot \mathbf{u}) (P^{-1})_{rs} (\mathbf{J}_s \cdot \mathbf{u}) \\ &= \left(\frac{\mathcal{J}^2}{ne \mathcal{P}} \right) \sum_{r, s=0}^N \lambda_r \delta_{rs}^{-1} \lambda_s. \end{aligned} \quad (12)$$

Here δ_{rs}^{-1} is the reciprocal of the matrix δ of elements δ_{rs} . The last factor in parenthesis is a characteristic function of this model and has dimensions of mobility. This will be here called $\bar{\mu}$:

$$\frac{\mathcal{J}^2}{ne \mathcal{P}} \equiv \bar{\mu} = \frac{3\gamma (KT)^{3/2} e^z - 1}{2^{7/2} \pi^{1/2} e m^{3/2} e^{1/2z}}. \quad (13)$$

The mobility formula can then be written as

$$\mu^{(N)} = \bar{\mu} F^{(N)}; \quad F^{(N)} \equiv \sum_{r, s=0}^N \lambda_r \delta_{rs}^{-1} \lambda_s. \quad (14)$$

In this way, the successive approximations evaluate to different orders a dimensionless function $F(z)$, whose relationship to Howarth and Sondheimer's function is

$$F(z) = \frac{16}{9\pi} - z e^{3/2z} e^{-z} G(z). \quad (15)$$

The result can be finally expressed in terms of Bessel functions,¹¹ which are tabulated and have known asymptotic expansions. The functions $G^{(0)}$ and $G^{(1)}$ are given by Howarth and Sondheimer. To second order one obtains from (14)

to study the sequence

$$F^{(0)} = \frac{z}{2}; \quad F^{(1)} = \frac{9}{16} z; \quad F^{(2)} = \frac{217}{384} z - \frac{217}{216} z^2 \equiv F^{(1)} \quad (16)$$

in the high-temperature limit.

¹¹ G. N. Watson, *A Treatise on the Theory of Bessel Functions* (Cambridge University Press, New York, 1922), p. 172.

This means that

$$\mu^{(2)} \approx 1.01\mu^{(1)} \approx 1.13\mu^{(0)} \quad (z \ll 1). \quad (17)$$

Thus, a zeroth-order approximation gives the correct temperature dependence and is very close in numerical value to the exact² result $F = z16/9\pi$, which is almost equal to $F^{(2)}$.

In low temperatures one obtains

$$F^{(0)} = \frac{z^{1/2}e^{3z}}{\pi^{1/2}}; \quad F^{(1)} = \frac{2z}{3}F^{(0)}; \quad F^{(2)} = F^{(1)}. \quad (18)$$

Thus,

$$\mu^{(2)} = \mu^{(1)} = \frac{2z}{3}\mu^{(0)} \gg \mu^{(0)} \quad (z \gg 1). \quad (19)$$

The zeroth-order approximation is now very bad, while in first order one obtains the exact solution. The low-temperature mobility formula is then, from (18) and (14):

$$\mu = \frac{\chi(\hbar\omega)^{3/2}}{2^{5/2}\pi em^{3/2}}(e^z - 1). \quad (20)$$

This formula was also derived by Fröhlich¹ on the assumption of elastic resonance scattering. He obtained a constant relaxation time $\tau = (2\alpha\omega\mathcal{N})^{-1}$ which leads to Eq. (20). However, if one calculates the relaxation time for the momentum of the carrier (rather than for the distribution) one obtains exactly three times the above result.

The low-temperature mobility has been studied by a number of authors. In all treatments, even in "true polaron" theories, like that of Low and Pines,¹² the conclusion is that $\mu \propto (e^z - 1)$, as one would expect on physical grounds from the phonon density number. Recently, a mobility calculation has been performed¹³ using Feynman's model¹⁴ of the polaron. This is perhaps the best calculation so far performed for high applied frequencies, and it contains some interesting predictions for high α . However, the authors derived the dc mobility by taking the limit of zero frequency, and thus concluded that $\mu \propto (e^z - 1)/z$. One would expect the results of a polaron theory to agree in the weak-coupling limit with the dc mobility obtained from the Boltzmann equation. The sequence of approximations shown in Eqs. (18) and (19) is interesting because it shows that a formula going like $(e^z - 1)/z$ is obtained in zeroth order, which is known to be a bad approximation in this region ($z \gg 1$), although it is quite good in high temperatures. The next approximation restores the simple exponential law for $z \gg 1$ by introducing the factor $2z/3$. Indeed, Kadanoff¹⁵ has recently reconsidered the Feynman model for the dc mobility and derived a result, valid in the low-temperature limit, which introduces precisely the factor $2z/3$.

¹² F. E. Low and D. Pines, Phys. Rev. **98**, 297 (1953).

¹³ R. P. Feynman, R. W. Hellwarth, C. K. Iddings, and P. M. Platzmann, Phys. Rev. **124**, 1007 (1962).

¹⁴ R. P. Feynman, Phys. Rev. **97**, 660 (1955).

¹⁵ L. P. Kadanoff (private communication).

The low-temperature region is very interesting for a physical discussion of the principles involved in the theory, but the experimental data are usually beset by all kinds of complications, such as additional scattering mechanisms and trapping of the carriers. Experimentally, the best region is often that of intermediate temperatures, which is theoretically difficult. The possibility of performing calculations at arbitrary temperatures is an attractive feature of the weak-coupling model. It has often been claimed that this theory is not subject to any restrictions in temperature and is valid for arbitrary values of z . Upon reflection, this is not very obvious. One could support by physical arguments the idea that this model, while valid in very low and very high temperatures, might be unjustifiable, or at least at its worst, when T is close to Θ . It is, perhaps, more reasonable to regard the practical feasibility, rather than its justification, as the virtue of the model. With this proviso, one can perform the calculations at arbitrary temperature with formulas (16) and (17) and the calculated values of $F(z)$. The results of the present computation (Table III), performed to high accuracy with a digital computer, reproduce the numerical estimates of Howarth and Sondheimer in high and low temperatures, but yield somewhat higher values in the region $1 < z < 2$.

For purposes of comparison of theory with experiment, it is necessary to first obtain a characteristic plot of the material: z versus T . Similarly, a second characteristic plot giving $\bar{\mu}$ versus z can be evaluated. In so doing, the mass parameter contained in $\bar{\mu}$ should be carried through. By definition, in this "nonpolaron" theory m is the crystal band mass of the electron. For not too strong coupling, the polaron mass m^* is given approximately by $m^* = m(1 + \alpha/6)$. This can be derived, for example, from the low-temperature theory of Lee, Low, and Pines.¹⁶ Using a free-energy analysis, Yokota¹⁷ attempted to extend this theory to include finite temperature effects, and concluded that

$$m^* = m \left[1 + \frac{\alpha}{6(2\mathcal{N} + 1)^{3/2}} \right], \quad (21)$$

which introduces a negligible correction at low temperatures ($\mathcal{N} \ll 1$) but affects m^* considerably by making it lighter as T increases. Van Heyningen's work¹⁸ shows that the Low-Pines low-temperature formula, when corrected with the Yokota factor, fits fairly well the observed drift mobility in AgCl from about 50°K ($z = 5.5$) to 300°K ($z = 0.77$).

In a purely heuristic manner, one might hope that the weak coupling theory is acceptable up to higher values of α if m is simply substituted by m^* . (In the same spirit, one might hope that the Yokota factor could help beyond the low temperature region.) To be

¹⁶ T. D. Lee, F. E. Low, and D. Pines, Phys. Rev. **90**, 297 (1953).

¹⁷ T. Yokota, Busseiron Kenkyo **69**, 137 (1953).

¹⁸ R. van Heyningen, Phys. Rev. **128**, 2112 (1962).

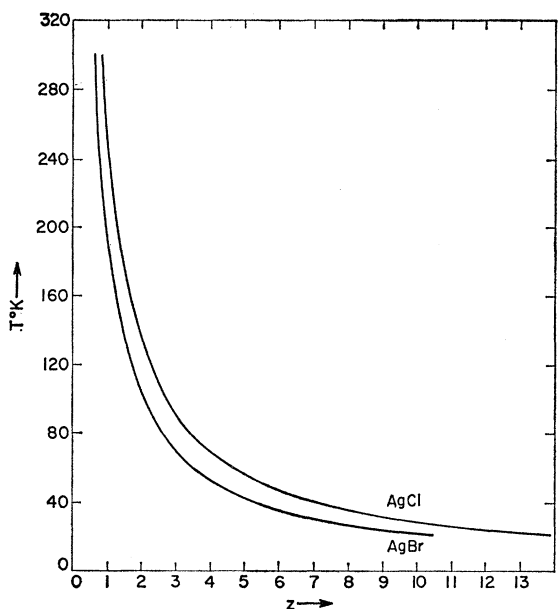


FIG. 1. Plot of z vs T for AgBr and AgCl.

sure, this is an incorrect procedure, equivalent to re-normalizing the mass but not the coupling constant. There is no *a priori* reason why such a procedure should work well, and one would expect it to be worse, the higher α is. In so doing, one is roughly postulating a model of carriers which behave rather like polarons in their (heavier) inertial response to the driving force, while behaving rather like electrons in a time average over their complicated scattering events.

AgCl and AgBr seem to have standard conduction band structures^{9,19} and the free carrier concentration in actual samples is sufficiently low to make the free carrier screening correction⁵ quite negligible. Thus, they constitute good materials to study the unmasked effects of the size of α (≈ 2). Also, samples can be prepared in which polar scattering seems to be fairly well established²⁰ over a wide temperature range. Given the interesting size of α in these materials it was thought worthwhile to perform a semiempirical mobility calculation for the experimental temperature range using Yokota's polaron mass in formula (13).

From experimental data on the reststrahl frequency ω , by Jones *et al.*,²¹ and from dielectric constant measurements by Eucken and Büchner²² at different temperatures one can evaluate $\omega = (\epsilon_s/\epsilon_\infty)^{1/2}\omega_t$ as a slowly varying function of T . Thus, the first characteristic plot (Fig. 1) was obtained for AgBr and AgCl. Next,

¹⁹ G. Ascarelli and F. C. Brown, Phys. Rev. Letters **9**, 209 (1962).

²⁰ D. C. Burnham, F. C. Brown, and R. S. Knox, Phys. Rev. **119**, 1560 (1960).

²¹ G. O. Jones, D. H. Martin, P. A. Mawer, and C. H. Perry, Proc. Roy. Soc. (London) **A261**, 10 (1961).

²² A. Eucken and A. Büchner, Z. Physik. Chem. (Leipzig) **B27**, 343 (1934).

one can evaluate $\bar{\mu}$ as a function of z . In the present calculation the polaron mass (21) carries with it the crystal band mass m . This parameter was adjusted by fitting the observed drift mobility in the way which will be explained below. The second characteristic plot (Fig. 2) was obtained with the values of m thus adjusted. For the reasons explained in Sec. IV, only drift mobility data were considered, discarding low-field Hall mobility measurements.

In AgCl, very good data exist due to Haynes and Shockley²³ and to van Heyningen.¹⁸ The latter also estimated the mass parameter needed to fit his data with different theories. He found that Howarth and Sondheimer's weak-coupling formula was unable to explain the experimental results over the whole temperature range of the measurements. The curve calculated by van Heyningen using the Howarth-Sondheimer formula is reproduced for comparison in Fig. 3 (dotted line). The full line is the result of the present calculation introducing the Yokota polaron mass instead of the crystal band mass m in Eq. (13). The mass m is then contained in the mobility formula in a more complicated fashion, as it also enters into the definition of α and is regarded as an adjustable parameter. Its value, given in line (b) of Table I, was obtained by adjusting

TABLE I. Mass parameters (in units of m_e) estimated from experimental data on the drift mobility of electrons in AgCl. Low-temperature values for m^* and α . In case (a) no m^* would be contained in the model. The tabulated value is simply $m(1+\alpha/6)$.

| | m | m^* | α |
|------------------|------|--------|----------|
| (a) ^a | 0.48 | (0.67) | 2.4 |
| (b) ^b | 0.35 | 0.47 | 2.1 |
| (c) ^c | 0.29 | 0.39 | 1.9 |

^a Howarth-Sondheimer formula (reference 18).

^b Present calculation.

^c Low-Pines-Yokota formula (reference 18).

the formula to fit the experimental data on the low-temperature side. This results in quite a good agreement with the data around room temperature. The worst

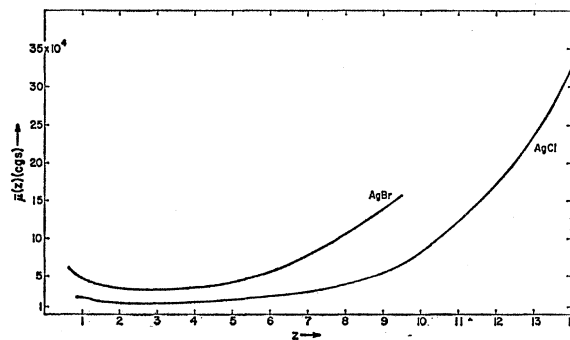


FIG. 2. The function μ vs z , evaluated using the Yokota mass m^* instead of m , and taking $m = 0.26 m_e$ for AgBr and $m = 0.35 m_e$ for AgCl.

²³ J. R. Haynes and W. Shockley, Phys. Rev. **82**, 935 (1951).

discrepancy with experiment amounts to about 30% and takes place when $T \lesssim \Theta$. As argued above, this is the region in which one has least trust in the calculation. This, however, might well be fortuitous and could arise to some extent from poor data, derived from old measurements of the dielectric constants. Table I also shows that the mass parameter derived in the present calculation is appreciably lower than that obtained with the Howarth-Sondheimer formula, and closer to the values estimated by van Heyningen using formulas based on intermediate coupling models for the polaron mobility.

In AgBr, drift mobility data are available²⁴ between about 77° and 200°K. When extrapolated to 300°K, they tend to agree with isolated measurements performed by other authors^{25,26} at that temperature. However, the data so far available are not as good as in AgCl. They show appreciable spread among themselves and, on the low-temperature side, they soon tend to level off, possibly due to shallow trapping effects. On the other hand, the effective mass is now known experimentally from the cyclotron resonance work of Ascarelli and Brown,¹⁹ which presumably measures the low-temperature polaron mass.

Figure 4 shows the experimental mobility data for AgBr and two alternative theoretical curves obtained

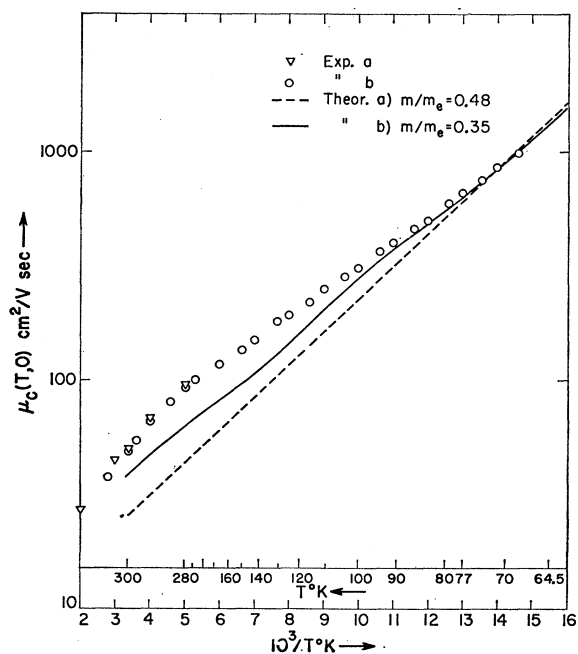


FIG. 3. Temperature dependence of the drift mobility of electrons in AgCl. Exp a: Haynes and Shockley. Exp b: van Heyningen. Theor a: Calculated by van Heyningen using the Howarth-Sondheimer formula. Theor b: present calculation.

²⁴ L. Chollet and J. Rossel, *Helv. Phys. Acta* **32**, 476 (1959); **33**, 627 (1960).

²⁵ J. Irmer and P. Süptitz, *Phys. Status Solidi* **1**, 481 (1961).

²⁶ C. Yamanaka, M. Saki, and T. Suita, *J. Phys. Soc. Japan* **11**, 605 (1956).

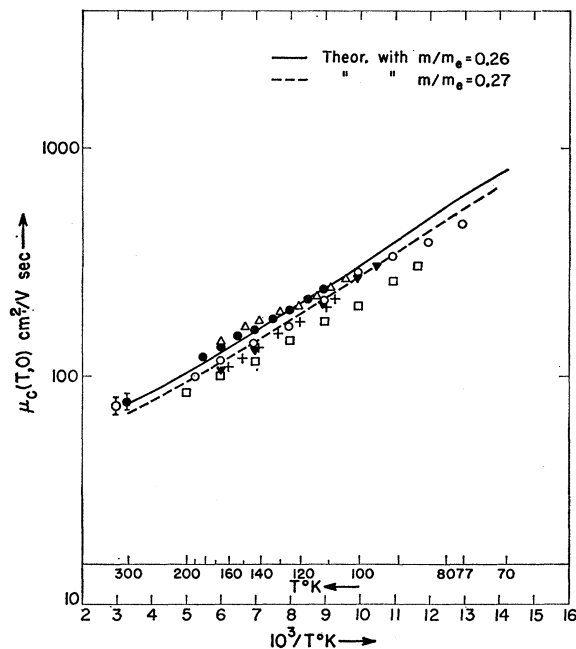


FIG. 4. Temperature dependence of the drift mobility of electrons in AgBr. Theoretical curves: Present calculation, with two different values of m/m_e . Experimental data: +, Δ , ∇ , \bullet , \square , and \circ : Chollet-Rossel, 1959 and 1960, different samples; \bullet with error flags, Irmer-Süptitz; \circ with error flags, Yamamaka-Sakai-Suita.

in the present calculation. The calculation was done again using the Yokota polaron mass as for AgCl. The full line was adjusted to pass through some of the data reported by Chollet and Rossel,²⁴ so as to fit the room-temperature measurements by the other authors.^{25,26} This resulted in a value of the mass parameter which overestimates the experimental mass by about 24%. It is perhaps more reasonable to compromise with the lower mobility data. This was done in the dotted line, at the expense of overestimating the cyclotron resonance mass by about 31% (Table II, line b).

TABLE II. Mass parameters (in units of m_e) estimated from experimental data on the drift mobility of electrons in AgBr. Low-temperature values for m^* and α . In case (a) the value of m^* means simply $m(1+\alpha/6)$.

| | m | m^* | α |
|------------------|------|--------|----------|
| (a) ^a | 0.43 | (0.60) | 2.3 |
| (b) ^b | 0.27 | 0.35 | 1.9 |
| (c) ^c | 0.30 | 0.39 | 2.0 |
| Exp ^d | | 0.27 | |

^a Howarth-Sondheimer formula adjusted to low-temperature data only (reference 19).

^b Present calculation.

^c Low-Pines formula adjusted to low-temperature data only (reference 19).

^d Mass derived from cyclotron resonance (reference 19).

The above numbers could still be improved, for example, by including terms of order α^2 in the polaron mass. This, however, is not the purpose of this work. The main lesson from these numerical estimates seems

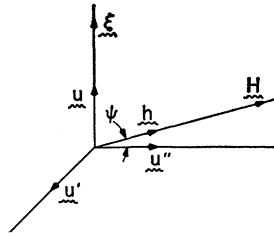


FIG. 5. Geometry for magnetoconductivity analysis.

to be that a simple-minded use of the Boltzmann equation and perturbation theory works fairly well up to higher values of α than allowed by the weak coupling criterion. If m^* is simply used instead of m , it seems reasonable to expect quite good results up to $\alpha \sim 1$. This makes it worthwhile studying the properties of the model in detail.

III. THE TRANSPORT COEFFICIENTS IN A MAGNETIC FIELD

This section is devoted to the phenomenological aspects of the type of measurements in which $\boldsymbol{\varepsilon}$ is fixed. The vectors of interest are $\boldsymbol{\varepsilon} = \varepsilon \mathbf{u}$, $\mathbf{H} = H \mathbf{h}$ and $\mathbf{J} = \boldsymbol{\sigma} \cdot \boldsymbol{\varepsilon}$, which can be expressed in any system of axes in the crystal. It is convenient to consider the orthogonal set \mathbf{u} , \mathbf{u}' , \mathbf{u}'' of Fig. 5, defined so that $\mathbf{u}' \perp \mathbf{h}$. With $\boldsymbol{\varepsilon}$ fixed, the experiment amounts to measuring the components $\mathbf{u} \cdot \mathbf{J} = \mathbf{u} \cdot \boldsymbol{\sigma} \cdot \mathbf{u} \boldsymbol{\varepsilon}$; $\mathbf{u}' \cdot \mathbf{J} = \mathbf{u}' \cdot \boldsymbol{\sigma} \cdot \mathbf{u} \boldsymbol{\varepsilon}$; $\mathbf{u}'' \cdot \mathbf{J} = \mathbf{u}'' \cdot \boldsymbol{\sigma} \cdot \mathbf{u} \boldsymbol{\varepsilon}$ (22)

Each component has a transport coefficient associated with it. For an isotropic gas of carriers in a magnetic field perpendicular to the electric field the quantity $\mathbf{u} \cdot \mathbf{J}''$ vanishes.

The transport coefficient associated with $\mathbf{u} \cdot \mathbf{J}$ is the *conductivity mobility*, μ_c :

$$\mu_c = (ne)^{-1} \frac{\mathbf{u} \cdot \mathbf{J}}{\boldsymbol{\varepsilon}} = \mathbf{u} \cdot \boldsymbol{\mu} \cdot \mathbf{u}; \quad \boldsymbol{\mu} = (ne)^{-1} \boldsymbol{\sigma}. \quad (23)$$

Here, $\boldsymbol{\mu}$ is the mobility tensor, which does not depend on the carrier concentration. For $H=0$, the coefficient μ_c is termed the drift mobility μ , as in Sec. II.

The second quantity of experimental interest is the Hall angle θ_H , defined by

$$\tan \theta_H = \frac{\mathbf{u}' \cdot \mathbf{J}}{\mathbf{u} \cdot \mathbf{J}} = \frac{\mathbf{u}' \cdot \boldsymbol{\mu} \cdot \mathbf{u}}{\mathbf{u} \cdot \boldsymbol{\mu} \cdot \mathbf{u}}.$$

From this one can define the *Hall mobility*, μ_H by

$$\tan \theta_H = \frac{\mu_H H}{c}; \quad \mu_H = \frac{c}{H} \frac{\mathbf{u}' \cdot \boldsymbol{\mu} \cdot \mathbf{u}}{\mathbf{u} \cdot \boldsymbol{\mu} \cdot \mathbf{u}}. \quad (24)$$

Since $\mathbf{u}' \cdot \boldsymbol{\mu} \cdot \mathbf{u}$ and $\mathbf{u} \cdot \boldsymbol{\mu} \cdot \mathbf{u}$ are invariant scalars, one can conveniently choose the reference frame to evaluate these formulas.

The transport coefficients in the more conventional type of measurements (where \mathbf{J} is fixed) are the re-

sistivity ρ and Hall coefficient R . It is easy to relate them to the two mobilities. One finds

$$\rho = \frac{1}{ne\mu_c [1 + (\mu_H H/c)^2]};$$

$$R = -\frac{1}{nec} \left(\frac{\mu_H}{\mu_c} \right) \frac{1}{1 + (\mu_H H/c)^2}. \quad (25)$$

The second relationship will be considered in the next section.

Now consider the nondispersive model, with constant isotropic τ and m . The simplest choice of axes is that for which $\mathbf{u} = (1,0,0)$ and $\mathbf{u}' = (0,1,0)$. The elements of the mobility tensor are then

$$\mu_{11} = \frac{\mu}{1 + (\mu H/c)^2} = \mu_{22};$$

$$\mu_{12} = \frac{\mu^2 H/c}{1 + (\mu H/c)^2} = -\mu_{21}; \quad \mu = \frac{e\tau}{m}. \quad (26)$$

Then, from (23) and (24),

$$\mu_c = \frac{\mu}{1 + (\mu H/c)^2}; \quad \mu_H = \mu = \frac{e\tau}{m}. \quad (27)$$

Thus, there is a *magnetoconductivity* effect but the Hall mobility is equal to the drift mobility at all fields. However, from (25):

$$\rho = \frac{1}{ne\mu}; \quad R = -\frac{1}{nec}. \quad (28)$$

The second equality is just the counterpart of the statement $\mu_H = \mu$. The first equation means that, for the nondispersive model (constant τ and m) there is no magnetoresistivity.

The above considerations show that the difference between a dispersive and a nondispersive model is more subtle in magnetoconductivity terms than in magnetoresistivity terms. A study of this question requires a detailed evaluation of the mobility tensor for the dispersive model and an examination of its properties in terms of μ_c and μ_H . This is done in the following section.

IV. MOBILITY CALCULATIONS IN A MAGNETIC FIELD

Equation (4) expresses the fact that an electric field applied along a direction \mathbf{u} upsets the equilibrium distribution by imparting an amount of drift momentum in the direction \mathbf{u} , to an extent measured by the function φ . If a magnetic field is present in an arbitrary direction \mathbf{h} (Fig. 5), one expects drift momentum to be imparted along \mathbf{u} , \mathbf{u}' and \mathbf{u}'' , by various amounts given by functions φ , φ' , and φ'' , respectively. The expansion of Φ_k

in the N th approximation becomes then

$$\Phi_{\mathbf{k}}^{(N)} = \sum_{r=0}^N c_r \mathbf{u} \cdot \mathbf{k} E^r + \sum_{r'=0}^N c_{r'} \mathbf{u}' \cdot \mathbf{k} E^{r'} + \sum_{r''=0}^N c_{r''} \mathbf{u}'' \cdot \mathbf{k} E^{r''}. \quad (29)$$

This can be written as

$$\Phi_{\mathbf{k}}^{(N)} = \sum_{\rho=0}^{3N+2} b_{\rho} \psi_{\rho} \quad (30)$$

with the convention that b_{ρ} and ψ_{ρ} correspond to the c_r and φ_r in Eq. (4) with the appropriate number of primes as one spans the total set $\{\psi_{\rho}\}$.

The magnetic field is represented in the transport equation by the magnetic operator

$$\hat{M} = -\frac{e}{\hbar c} \frac{\partial f_{\mathbf{k}}^0}{\partial E} (\mathbf{v} \times \mathbf{H}) \cdot \nabla_{\mathbf{k}}.$$

The equation to be solved is then

$$\hat{L} \Phi_{\mathbf{k}} \equiv (\hat{P} + M) \Phi_{\mathbf{k}} = -e \frac{\partial f_{\mathbf{k}}^0}{\partial E} \mathbf{v} \cdot \mathbf{u} \mathcal{E}.$$

The way in which the variational principle is extended to this equation is explained in Ziman's book¹⁰ (Chap. 12). The "entropy production" $\langle \Phi_{\mathbf{k}} | \hat{L} \Phi_{\mathbf{k}} \rangle$ does not obey a maximum principle because the operator \hat{M} is antisymmetric or, more physically, because the Lorentz force does not perform work explicitly. While not having a definite sign, one can still establish a variational principle for a modified expression of the form $\frac{1}{2} \{ \langle \Phi_{\mathbf{k}}^* | \hat{L} \Phi_{\mathbf{k}} \rangle + \langle \Phi_{\mathbf{k}} | \hat{L}^* \Phi_{\mathbf{k}}^* \rangle \}$, where conjugation would formally correspond to inversion of the magnetic field. This expression becomes equal to the standard rate of entropy production once the steady state has been reached. By this device, independent variation of $\Phi_{\mathbf{k}}^*$ yields a Boltzmann equation for $\Phi_{\mathbf{k}}$ and vice versa.

In a practical application of the method, one determines the coefficients b_{ρ} of the expansion of $\Phi_{\mathbf{k}}^{(N)}$, Eq. (30) by the resulting variational equations, which constitute a formal extension of Eqs. (8), and are

$$\sum_{\sigma} L_{\rho\sigma} b_{\sigma} = \mathbf{J}_{\sigma} \cdot \mathbf{u} \mathcal{E}. \quad (31)$$

Lewis and Sondheimer⁸ made a first attempt to study the transport problem with polar scattering in a magnetic field. Their work was restricted to the isotropic model under consideration and to the case $\mathbf{H} \perp \boldsymbol{\varepsilon}$. Then they used the well-known device of employing the complex rotation in the plane of $\boldsymbol{\varepsilon}$ and $\boldsymbol{\varepsilon} \times \mathbf{H}$. (This device would not be so obvious in a more general case, where the third dimension has to be explicitly considered. Instead, an algebraic method will be presently proposed to include the three dimensional case.) In

their notation, Lewis and Sondheimer expanded the function $\Phi_{\mathbf{k}}$ in a form equivalent to Eq. (30) (without a term in \mathbf{u}'') and used, purely on the grounds of plausibility, a set of equations similar to Eq. (31) of this paper. For the case $\mathbf{H} \perp \boldsymbol{\varepsilon}$ of the scheme developed here, Lewis and Sondheimer's results turn out to be equivalent to the results of the present calculation to a first-order approximation. This point will be mentioned again.

Now with the method of calculation. With the same notation as in Sec. II, the matrix terms P_{rs} are substituted by $L_{\rho\sigma} = P_{\rho\sigma} + M_{\rho\sigma}$. These then form a matrix with $3(N+1)$ rows and columns. It is easily seen from symmetry considerations that the operator \hat{P} only has matrix terms between functions of the same subset. It is practical to think of the $3(N+1)$ by $3(N+1)$ matrix as a 3×3 supermatrix whose elements are matrices of $(N+1)$ rows and columns. The supermatrix of \hat{P} is then diagonal and the three diagonal elements are equal to the $(N+1)$ by $(N+1)$ matrix P of Sec. II, i.e.,

$$\|P_{\rho\sigma}\| = \begin{pmatrix} P & 0 & 0 \\ 0 & P & 0 \\ 0 & 0 & P \end{pmatrix}.$$

From the structure of the operator \hat{M} it is also seen by symmetry considerations that it only has matrix terms between functions of different subsets. Specifically, the supermatrix of \hat{M} takes the "off-diagonal," antisymmetric form

$$\|M_{\rho\sigma}\| = \begin{pmatrix} 0 & M \cos\psi & 0 \\ -M \cos\psi & 0 & -M \sin\psi \\ 0 & M \sin\psi & 0 \end{pmatrix}.$$

Here, M is a $(N+1)$ by $(N+1)$ matrix of elements given by

$$\begin{aligned} \cos\psi M_{ij} &\equiv \langle \varphi_i | \hat{M} \varphi_j' \rangle \\ &= \frac{eH \cos\psi}{mc} \int (\mathbf{u} \cdot \mathbf{k})^2 \frac{\partial f_{\mathbf{k}}^0}{\partial E} E^{i+j} d\mathbf{k}. \end{aligned} \quad (32)$$

In this scheme M is clearly a symmetric matrix. Transforming (31) to an integration over energy, the M_{ij} 's can be written as follows:

$$M_{ij} = \mathfrak{N}(KT)^{i+j} \Gamma_{ij},$$

where

$$\Gamma_{ij} = \frac{\Gamma(i+j+\frac{5}{2})}{\Gamma(\frac{5}{2})}; \quad \mathfrak{N} = -\frac{\mu \mathbf{H} \cdot \mathbf{u}''}{c} = -\phi Y. \quad (33)$$

The second equality defines the dimensionless variable Y .

The calculations are greatly simplified by the fact that the supermatrix is blocked off in matrices which are only P or only M . This provides a natural way to disentangle M and P for arbitrary orientation of \mathbf{H} . Moreover, the scalars $\mathbf{J}_\sigma \cdot \mathbf{u}$ of Eq. (31) are obtained from the same vector integral of (10) with the corresponding function ψ_ρ . Again, for symmetry reasons, this is zero unless ψ_ρ is one of the functions φ_r of the first subset. This simplifies further the evaluation of the transport coefficients. The mobility tensor in the N th-order approximation, obtained from Eq. (31) is

$$\mathbf{u} = \mathbf{u}(\mathbf{H}) = \frac{1}{ne} \sum_{\rho, \sigma=0}^N \mathbf{J}_\rho L_{\rho\sigma}^{-1} \mathbf{J}_\sigma. \quad (34)$$

In order to invert the supermatrix L one simply has to solve the set of linear algebraic equations which arise from the condition that LL^{-1} must give the unit supermatrix, i.e., if I is the unit matrix of $(N+1)$ rows and columns:

$$\begin{pmatrix} P & M \cos\psi & 0 \\ -M \cos\psi & P & -M \sin\psi \\ 0 & M \sin\psi & 0 \end{pmatrix} \begin{pmatrix} A & B & C \\ -B & D & E \\ -C & -E & F \end{pmatrix} = \begin{pmatrix} I & 0 & 0 \\ 0 & I & 0 \\ 0 & 0 & I \end{pmatrix}. \quad (35)$$

The resulting set of linear equations for the unknown matrices A, B, \dots, F is easily solved by an obvious extension of the procedure one would use with ordinary numbers and the unknown matrices can then be written in terms of P, P^{-1}, M , and M^{-1} . The matrix P was already inverted in the study of the problem for $H=0$, and the matrix M is essentially a matrix of gamma functions and is much easier to handle.

Furthermore, it is unnecessary to know all the matrices of L^{-1} . For the magnetoconductivity measurements one is interested in the three scalars $\mathbf{u} \cdot \mathbf{u} \cdot \mathbf{u}$, $\mathbf{u}' \cdot \mathbf{u} \cdot \mathbf{u}$, and $\mathbf{u}'' \cdot \mathbf{u} \cdot \mathbf{u}$. The vectors \mathbf{J}_ρ only have components on \mathbf{u} , \mathbf{u}' , and \mathbf{u}'' , for ψ_ρ belonging to $\{\varphi_r\}$, $\{\varphi'_{r'}\}$, and $\{\varphi''_{r''}\}$, respectively. It follows that

$$\begin{aligned} \mathbf{u} \cdot \mathbf{u}^{(N)} \cdot \mathbf{u} &= \frac{1}{ne} \sum_{r, s=0}^N \mathbf{J}_r \cdot \mathbf{u} A_{rs} \mathbf{J}_s \cdot \mathbf{u}, \\ \mathbf{u}' \cdot \mathbf{u}^{(N)} \cdot \mathbf{u} &= \frac{1}{ne} \sum_{r, s=0}^N \mathbf{J}_r \cdot \mathbf{u} B_{rs} \mathbf{J}_s \cdot \mathbf{u}, \\ \mathbf{u}'' \cdot \mathbf{u}^{(N)} \cdot \mathbf{u} &= \frac{1}{ne} \sum_{r, s=0}^N \mathbf{J}_r \cdot \mathbf{u} C_{rs} \mathbf{J}_s \cdot \mathbf{u}. \end{aligned} \quad (36)$$

Thus, it is only necessary to know three matrices of L^{-1} , namely, A, B , and C .

Having established how the calculation can be done for arbitrary angle between \mathbf{H} and $\boldsymbol{\varepsilon}$, the formulas will now be evaluated for $\mathbf{H} \perp \boldsymbol{\varepsilon}$. Then $\cos\psi=1$ and the solution of (35) is

$$A = (MS)^{-1}; \quad B = -(PS)^{-1}; \quad S = P^{-1}M + M^{-1}P. \quad (37)$$

From (23), (24), (36), and (37), the two mobilities are, in the N th approximation,

$$\begin{aligned} \mu_c^{(N)} &= \frac{1}{ne} \sum_{r, s=0}^N \mathbf{J}_r \cdot \mathbf{u} (MS)_{rs}^{-1} \mathbf{J}_s \cdot \mathbf{u}, \\ \mu_H^{(N)} &= \frac{\sum_{r, s=0}^N \mathbf{J}_r \cdot \mathbf{u} (PS)_{rs}^{-1} \mathbf{J}_s \cdot \mathbf{u}}{H ne \mu_c^{(N)}}. \end{aligned} \quad (38)$$

From the elements δ_{rs} and Γ_{rs} , one has the dimensionless matrices δ, Γ and their reciprocals. Changing from the physical variables (T, H) to the dimensionless variables (z, Y) one can define the dimensionless matrix

$$\nu \equiv \Gamma^{-1} \delta + Y^2 \delta^{-1} \Gamma = \nu(z, Y). \quad (39)$$

It will be remembered that, in this case, $Y = \bar{\mu}H/c$. Recalling Eqs. (7), (8), (13), and (32) one can finally write the two mobilities in the form

$$\mu_c = \bar{\mu} F_c(z, Y); \quad \mu_H = \bar{\mu} F_H(z, Y), \quad (40)$$

where in the N th approximation,

$$\begin{aligned} F_c^{(N)}(z, Y) &= \sum_{r, s=0}^N \lambda_r (\Gamma \nu)^{-1} \lambda_s = (\Gamma \nu^{-1})_{00}^{(N)} \\ F_H^{(N)}(z, Y) &= \frac{\sum_{r, s=0}^N \lambda_r (\delta \nu)^{-1} \lambda_s}{F_c^{(N)}(z, Y)} = \frac{(\Gamma \nu^{-1} \delta^{-1} \Gamma)_{00}^{(N)}}{(\Gamma \nu^{-1})_{00}^{(N)}}. \end{aligned} \quad (41)$$

The last equalities follow from the fact that $\lambda_r = \Gamma_{r0}$. When $H=0$, $F_c(z, 0)$ is the function $F(z)$ of Sec. II.

It is trivial to see that Eqs. (40) read the same as Eqs. (27) of the nondispersive model only if the functions of (41) are evaluated to lowest order. But it was seen in Sec. II that this is a bad approximation, except at very high temperatures. This approximation, on the other hand, is exact in the limit of very high magnetic fields. If one ignores quantization effects, this is to be expected on physical grounds: in very high fields the details of the scattering become relatively unimportant. In this (high-field) limit, Eqs. (41) give

$$\begin{aligned} F_c^{(N)} &= Y^{-2} (\Gamma \Gamma^{-1} \delta)_{00}^{(N)} = \left(\frac{c}{\bar{\mu}H} \right)^2 \delta_{00}, \\ F_H^{(N)} &= Y^{-2} \frac{(\Gamma \Gamma^{-1} \delta \delta^{-1} \Gamma)_{00}^{(N)}}{(\Gamma \Gamma^{-1} \delta)_{00}^{(N)}} = \frac{1}{\delta_{00}}, \end{aligned} \quad (42)$$

showing that the zeroth approximation is, indeed, exact. A simple relationship holds then for the two mobilities, namely,

$$\mu_c \mu_H = \left(\frac{c}{H}\right)^2 \quad (H \rightarrow \infty). \quad (43)$$

From (15), this means that

$$-necR = 1 \quad (H \rightarrow \infty). \quad (44)$$

On the other hand, in the low-field limit one has from (41) that $\mu_H(z,0) \geq \mu_c(z,0)$, or $-necR(z,0) \geq 1$.

The low-field Hall mobility is a quantity of considerable experimental interest. Its ratio to the drift mobility was estimated by Lewis and Sondheimer, in the form $-necR(z,0)$. As explained above, their estimate is equivalent to the first-order approximation of the scheme developed in this paper. It will presently be seen that this approximation is still far from accurate, although it displays qualitatively the distinct features of the dispersive model. Delves²⁷ used a numerical procedure directly on the Boltzmann equation and estimated $-necR(z,0)$ for three isolated values of z . He obtained somewhat higher values than Lewis and Sondheimer.

The calculation outlined above was programmed for a digital computer to evaluate fully $F_c(z,Y)$ and $F_H(z,Y)$ to third order, i.e., with 4×4 matrices. From the two characteristic plots, $z(T)$ and $\bar{\mu}(z)$ one can read the dimensionless variables in terms of T and H for a given material. The ranges of z and Y were chosen so that, from representative values of $\bar{\mu}$ for AgBr and AgCl, they would correspond roughly to $20^\circ\text{K} \leq T \leq 300^\circ\text{K}$ and $0 \leq H \leq 6 \times 10^4$ G. Table III gives the results for values of z chosen so as to correspond to likely experimental conditions. The value of $z=10$ is also included to indicate the trend in the temperature dependence of the galvanomagnetic effects and for eventual comparison with the results of more advanced theories for stronger coupling. Obviously, low temperatures are required for the mobilities to be appreciably modified by the magnetic field. It is seen in Table III that, at $T = \Theta/3$, for the maximum values of Y which have been used the conductivity mobility only decreases by a few percent, and the Hall mobility still remains practically unchanged.

In order to look for the distinctive features of the dispersive model (e.g., an appreciable decrease in the Hall mobility) one should seek low temperatures, as much as possible, and effectively high magnetic fields. From Eqs. (42), a field intensity is effectively high for a material when $F_c F_H$ becomes comparable to Y^{-2} . From the data of Sec. II and Table III one would guess that this is roughly the case for AgCl at $T \approx 70^\circ\text{K}$ and $H = 6 \times 10^4$. Under these conditions one can probably ignore high-field quantum effects. Assuming $m = 0.4$

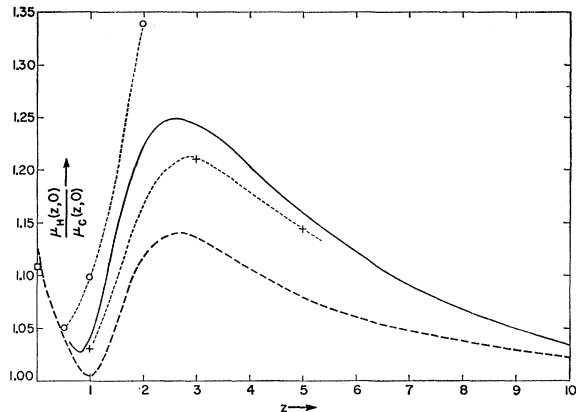


FIG. 6. Temperature dependence of the ratio $\mu_H(z,0)/\mu_c(z,0)$; \circ : Delves, numerical work; \square : Delves, assuming $\tau \propto E^{1/2}$. Dashed line: Lewis and Sondheimer, first-order approximation; $+$: Lewis and Sondheimer, second-order approximation. Full line: present work, third-order approximation.

m_e , the spacing between Landau levels can be estimated as 2.8×10^{-15} erg, which is to be compared with $KT = 9.7 \times 10^{-15}$ erg.

Table III also gives the values of $F_c(z,0)$, which can be compared through Eq. (15) with Howarth and Sondheimer's estimate for their function $e^{-\xi}G(z)$. The other quantity of experimental interest in low fields is $F_H(z,0)$, if one is interested in the low-field Hall mobility, or $F_H(z,0)/F_c(z,0)$, which gives $\mu_H(z,0)/\mu_c(z,0)$ as can be seen from Eq. (40). This ratio is plotted as a function of z in Fig. 6, where it is compared with previous estimates. It is seen that the convergence obtained with the power series expansion is fairly good in high and low temperatures, but is somewhat poor at intermediate temperatures. This is typically the bad region; it is also in this range that $F_c(z,0)$ turns out to be a few percent higher than in previous approximations.

Very little experimental work has been done so far to search for a check on the facts predicted in Fig. 6. Some support for this may be provided by the recent work of Halsted *et al.*²⁸ on CdTe. In this material the estimated value of α is 0.39, and the weak-coupling model should be appropriate. The authors of reference 28 measured the low-field Hall mobility over a certain temperature range. The drift mobility calculated with Howarth and Sondheimer's function turned out to be systematically lower. Delves' isolated points were used for an approximate interpolation to estimate the ratio $\mu_H(z,0)/\mu_c(z,0)$. When the calculated values of $\mu_c(z,0)$ were multiplied by this factor the result was larger in good agreement with experiment. Since the theoretical values of $\mu_c(z,0)$ are somewhat underestimated when the Howarth-Sondheimer function is used, the same result is compatible with a lowering of Delves' numerical values

²⁷ R. T. Delves, Proc. Phys. Soc. (London) **73**, 572 (1959).

²⁸ B. Segall, M. R. Lorenz, and R. E. Halsted, Phys. Rev. **129**, 2471 (1963).

TABLE III. The functions $F_c(z,Y)$ and $F_H(z,Y)$ evaluated to third-order approximation. The number following "E" indicates the power of 10 with which the preceding number is to be multiplied. The ratio $F_H(z,0)/F_c(z,0)$ is plotted in Fig. 6. The functions $F_c(z,Y)$ and $F_H(z,Y)$ can be used to compute the mobilities according to Eq. (40).

| Z | Z=3.0 | | Z=3.5 | | Z=4.0 | | | | | |
|-------|------------|----------|----------|----------|----------|----------|----------|----------|----------|----------|
| | $F_c(z,0)$ | Y | F_c | F_H | Y | F_c | Y | F_c | F_H | |
| 0.65 | 3.699E-1 | 5.359E-4 | 7.559E+0 | 9.407E+0 | 5.467E-4 | 1.248E+1 | 1.531E+1 | 5.823E-4 | 1.995E+1 | 2.400E+1 |
| 0.70 | 4.026E-1 | 1.072E-3 | 7.559E+0 | 9.407E+0 | 1.093E-3 | 1.248E+1 | 1.531E+1 | 1.164E-3 | 1.994E+1 | 2.400E+1 |
| 0.75 | 4.368E-1 | 2.144E-3 | 7.556E+0 | 9.407E+0 | 2.187E-3 | 1.247E+1 | 1.531E+1 | 2.329E-3 | 1.989E+1 | 2.400E+1 |
| 0.80 | 4.728E-1 | 3.215E-3 | 7.552E+0 | 9.407E+0 | 3.280E-3 | 1.245E+1 | 1.531E+1 | 3.494E-3 | 1.981E+1 | 2.400E+1 |
| 0.85 | 5.107E-1 | 4.287E-3 | 7.547E+0 | 9.406E+0 | 4.374E-3 | 1.243E+1 | 1.530E+1 | 4.656E-3 | 1.970E+1 | 2.399E+1 |
| 0.90 | 5.508E-1 | 5.359E-3 | 7.539E+0 | 9.406E+0 | 5.467E-3 | 1.239E+1 | 1.530E+1 | 5.823E-3 | 1.956E+1 | 2.398E+1 |
| 0.95 | 5.932E-1 | 6.431E-3 | 7.531E+0 | 9.405E+0 | 6.561E-3 | 1.235E+1 | 1.530E+1 | 6.987E-3 | 1.939E+1 | 2.398E+1 |
| 1.00 | 6.383E-1 | 7.503E-3 | 7.520E+0 | 9.405E+0 | 7.654E-3 | 1.231E+1 | 1.530E+1 | 8.152E-3 | 1.920E+1 | 2.397E+1 |
| 1.05 | 6.857E-1 | 8.575E-3 | 7.509E+0 | 9.404E+0 | 8.747E-3 | 1.226E+1 | 1.530E+1 | 9.316E-3 | 1.898E+1 | 2.396E+1 |
| 1.10 | 7.370E-1 | 9.646E-3 | 7.495E+0 | 9.403E+0 | 9.841E-3 | 1.220E+1 | 1.529E+1 | 1.048E-2 | 1.873E+1 | 2.394E+1 |
| 1.15 | 7.913E-1 | 1.072E-2 | 7.480E+0 | 9.402E+0 | 1.093E-2 | 1.213E+1 | 1.529E+1 | 1.164E-2 | 1.847E+1 | 2.393E+1 |
| 1.20 | 8.488E-1 | 1.179E-2 | 7.464E+0 | 9.401E+0 | 1.203E-2 | 1.206E+1 | 1.529E+1 | 1.281E-2 | 1.819E+1 | 2.391E+1 |
| 1.30 | 9.753E-1 | 1.286E-2 | 7.446E+0 | 9.400E+0 | 1.312E-2 | 1.198E+1 | 1.528E+1 | 1.397E-2 | 1.789E+1 | 2.390E+1 |
| 1.40 | 1.118E0 | 1.393E-2 | 7.426E+0 | 9.398E+0 | 1.421E-2 | 1.190E+1 | 1.528E+1 | 1.513E-2 | 1.757E+1 | 2.388E+1 |
| 1.60 | 1.462E0 | 1.500E-2 | 7.406E+0 | 9.397E+0 | 1.531E-2 | 1.181E+1 | 1.527E+1 | 1.630E-2 | 1.725E+1 | 2.386E+1 |
| 1.80 | 1.895E0 | 1.608E-2 | 7.384E+0 | 9.396E+0 | 1.640E-2 | 1.172E+1 | 1.527E+1 | 1.747E-2 | 1.691E+1 | 2.384E+1 |
| 2.00 | 2.436E0 | 1.715E-2 | 7.360E+0 | 9.394E+0 | 1.749E-2 | 1.162E+1 | 1.526E+1 | 1.863E-2 | 1.657E+1 | 2.382E+1 |
| 2.30 | 3.493E0 | 1.822E-2 | 7.335E+0 | 9.392E+0 | 1.859E-2 | 1.152E+1 | 1.525E+1 | 1.980E-2 | 1.621E+1 | 2.379E+1 |
| 2.60 | 4.917E0 | 1.929E-2 | 7.309E+0 | 9.390E+0 | 1.968E-2 | 1.142E+1 | 1.525E+1 | 2.096E-2 | 1.586E+1 | 2.377E+1 |
| 3.00 | 7.560E0 | 2.036E-2 | 7.281E+0 | 9.388E+0 | 2.077E-2 | 1.131E+1 | 1.524E+1 | 2.213E-2 | 1.550E+1 | 2.374E+1 |
| 3.50 | 1.248E+1 | 2.144E-2 | 7.253E+0 | 9.387E+0 | 2.187E-2 | 1.119E+1 | 1.523E+1 | 2.329E-2 | 1.514E+1 | 2.372E+1 |
| 4.00 | 1.995E+1 | 2.258E-2 | 7.191E+0 | 9.382E+0 | 2.405E-2 | 1.096E+1 | 1.522E+1 | 2.562E-2 | 1.442E+1 | 2.366E+1 |
| 5.00 | 4.767E+1 | 2.572E-2 | 7.126E+0 | 9.378E+0 | 2.624E-2 | 1.071E+1 | 1.520E+1 | 2.795E-2 | 1.371E+1 | 2.360E+1 |
| 5.50 | 7.151E+1 | 2.787E-2 | 7.056E+0 | 9.372E+0 | 2.843E-2 | 1.045E+1 | 1.518E+1 | 3.028E-2 | 1.302E+1 | 2.353E+1 |
| 6.00 | 1.059E+2 | 3.001E-2 | 6.982E+0 | 9.367E+0 | 3.062E-2 | 1.019E+1 | 1.516E+1 | 3.261E-2 | 1.236E+1 | 2.346E+1 |
| 6.50 | 1.550E+2 | 3.430E-2 | 6.823E+0 | 9.355E+0 | 3.499E-2 | 9.657E+0 | 1.512E+1 | 3.727E-2 | 1.111E+1 | 2.330E+1 |
| 7.00 | 2.247E+2 | 3.859E-2 | 6.653E+0 | 9.341E+0 | 3.936E-2 | 9.118E+0 | 1.507E+1 | 4.192E-2 | 9.981E+0 | 2.313E+1 |
| 7.50 | 3.228E+2 | 4.287E-2 | 6.472E+0 | 9.326E+0 | 4.374E-2 | 8.587E+0 | 1.502E+1 | 4.658E-2 | 8.981E+0 | 2.295E+1 |
| 8.00 | 4.603E+2 | 4.823E-2 | 6.237E+0 | 9.305E+0 | 4.920E-2 | 7.947E+0 | 1.494E+1 | 5.240E-2 | 7.899E+0 | 2.270E+1 |
| 8.50 | 6.519E+2 | 5.359E-2 | 5.995E+0 | 9.281E+0 | 5.467E-2 | 7.342E+0 | 1.486E+1 | 5.823E-2 | 6.982E+0 | 2.244E+1 |
| 9.00 | 9.179E+2 | 5.895E-2 | 5.750E+0 | 9.256E+0 | 6.014E-2 | 6.779E+0 | 1.477E+1 | 6.405E-2 | 6.206E+0 | 2.217E+1 |
| 10.00 | 1.303E+3 | 6.431E-2 | 5.505E+0 | 9.228E+0 | 6.560E-2 | 6.261E+0 | 1.468E+1 | 6.987E-2 | 5.549E+0 | 2.189E+1 |

which would bring them very close to the full line of Fig. 6. In any event, this experiment seems to support the idea that $\mu_H(z,0) \geq \mu_c(z,0)$, which is associated with dispersive behavior in a magnetic field. It would be interesting to see more work of this kind.

V. FINAL CONSIDERATIONS

From an over-all picture of the dc transport problem in terms of a weak-coupling model it seems that a more careful study of the galvanomagnetic properties would be highly desirable and informative. Better polaron theories should pay close attention to the question of dispersive behavior; so far, the models leading to a constant relaxation time have been mainly worked out for zero magnetic field and it might be that some of the physical arguments need revision when a magnetic field is present.

The experimental information so far available is often rather incomplete, its main weakness being lack of systematics. The temperature dependence of the low-field Hall coefficient still offers a wide scope for experimental work. Alternatively, the same worker should attempt to measure the two mobilities $\mu_c(z,0)$ and $\mu_H(z,0)$ for the same samples. In either case a wide temperature range should be interesting, going up to

$T > \Theta$. The challenge for the theories in the absence of a magnetic field is now in the intermediate temperature range. In planning magnetoconductivity experiments, it might be worthwhile making an effort to achieve effectively high magnetic fields. The field dependence of the Hall angle should be particularly interesting. A systematic program for galvanomagnetic measurements in AgBr and AgCl would provide very timely and relevant information.

Another aspect of the work described in this paper concerns the use of the variational techniques for practical calculations. The convergence, with the power series expansion, is very good in the two extreme limits $H=0$ and $H \rightarrow \infty$. However, it is rather slow at intermediate and low fields, as can be seen from the successive approximations to the Hall coefficient in Fig. 6. It is an open possibility that other variational methods, like the ones recently developed by Baylin²⁹ and Blount³⁰ might prove more practical, although this still has to be tested. The improvement of the convergence is probably to be sought rather in the expansion functions,

²⁹ M. Baylin, Phys. Rev. **126**, 2040 (1962).

³⁰ E. I. Blount (private communication).

TABLE III.—Continued.

| Z=5.0 | | | Z=5.5 | | | Z=10.0 | | |
|----------|----------|----------|----------|----------|----------|----------|----------|----------|
| Y | F_c | F_H | Y | F_c | F_H | Y | F_c | F_H |
| 6.769E-4 | 4.760E+1 | 5.533E+1 | 7.917E-4 | 7.120E+1 | 8.149E+1 | 3.000E-3 | 6.110E+1 | 1.733E+3 |
| 1.354E-3 | 4.739E+1 | 5.532E+1 | 1.583E-3 | 7.031E+1 | 8.145E+1 | 6.000E-3 | 1.585E+1 | 1.720E+3 |
| 2.708E-3 | 4.659E+1 | 5.529E+1 | 3.167E-3 | 6.694E+1 | 8.131E+1 | 1.200E-2 | 4.037E+0 | 1.700E+3 |
| 4.062E-3 | 4.532E+1 | 5.523E+1 | 4.750E-3 | 6.202E+1 | 8.108E+1 | 1.800E-2 | 1.826E+0 | 1.673E+3 |
| 5.415E-3 | 4.365E+1 | 5.515E+1 | 6.333E-3 | 5.628E+1 | 8.076E+1 | 2.400E-2 | 1.050E+0 | 1.638E+3 |
| 6.769E-3 | 4.169E+1 | 5.505E+1 | 7.917E-3 | 5.035E+1 | 8.037E+1 | 3.000E-2 | 6.902E-1 | 1.595E+3 |
| 8.123E-3 | 3.952E+1 | 5.493E+1 | 9.500E-3 | 4.468E+1 | 7.990E+1 | 3.600E-2 | 4.941E-1 | 1.548E+3 |
| 9.477E-3 | 3.725E+1 | 5.479E+1 | 1.108E-2 | 3.949E+1 | 7.937E+1 | 4.200E-2 | 3.755E-1 | 1.497E+3 |
| 1.083E-2 | 3.495E+1 | 5.464E+1 | 1.267E-2 | 3.490E+1 | 7.879E+1 | 4.800E-2 | 2.980E-1 | 1.444E+3 |
| 1.218E-2 | 3.268E+1 | 5.446E+1 | 1.425E-2 | 3.090E+1 | 7.817E+1 | 5.400E-2 | 2.446E-1 | 1.391E+3 |
| 1.354E-2 | 3.049E+1 | 5.426E+1 | 1.583E-2 | 2.745E+1 | 7.751E+1 | 6.000E-2 | 2.060E-1 | 1.338E+3 |
| 1.489E-2 | 2.840E+1 | 5.405E+1 | 1.742E-2 | 2.449E+1 | 7.683E+1 | 6.600E-2 | 1.770E-1 | 1.287E+3 |
| 1.625E-2 | 2.643E+1 | 5.383E+1 | 1.900E-2 | 2.194E+1 | 7.613E+1 | 7.200E-2 | 1.547E-1 | 1.238E+3 |
| 1.760E-2 | 2.460E+1 | 5.359E+1 | 2.058E-2 | 1.976E+1 | 7.542E+1 | 7.800E-2 | 1.370E-1 | 1.191E+3 |
| 1.895E-2 | 2.290E+1 | 5.334E+1 | 2.213E-2 | 1.787E+1 | 7.471E+1 | 8.400E-2 | 1.227E-1 | 1.147E+3 |
| 2.031E-2 | 2.134E+1 | 5.308E+1 | 2.375E-2 | 1.624E+1 | 7.400E+1 | 9.000E-2 | 1.109E-1 | 1.106E+3 |
| 2.166E-2 | 1.990E+1 | 5.281E+1 | 2.533E-2 | 1.482E+1 | 7.331E+1 | 9.600E-2 | 1.010E-1 | 1.067E+3 |
| 2.301E-2 | 1.859E+1 | 5.254E+1 | 2.692E-2 | 1.358E+1 | 7.262E+1 | 1.020E-1 | 9.254E-2 | 1.032E+3 |
| 2.437E-2 | 1.738E+1 | 5.225E+1 | 2.850E-2 | 1.249E+1 | 7.195E+1 | 1.080E-1 | 8.528E-2 | 9.990E+2 |
| 2.572E-2 | 1.628E+1 | 5.196E+1 | 3.008E-2 | 1.153E+1 | 7.130E+1 | 1.140E-1 | 7.896E-2 | 9.686E+2 |
| 2.708E-2 | 1.528E+1 | 5.166E+1 | 3.167E-2 | 1.067E+1 | 7.067E+1 | 1.200E-1 | 7.340E-2 | 9.406E+2 |
| 2.978E-2 | 1.351E+1 | 5.106E+1 | 3.483E-2 | 9.235E+0 | 6.947E+1 | 1.320E-1 | 6.408E-2 | 8.908E+2 |
| 3.249E-2 | 1.203E+1 | 5.046E+1 | 3.800E-2 | 8.073E+0 | 6.836E+1 | 1.440E-1 | 5.655E-2 | 8.484E+2 |
| 3.520E-2 | 1.077E+1 | 4.984E+1 | 4.117E-2 | 7.121E+0 | 6.735E+1 | 1.560E-1 | 5.035E-2 | 8.123E+2 |
| 3.791E-2 | 9.706E+0 | 4.925E+1 | 4.433E-2 | 6.330E+0 | 6.642E+1 | 1.680E-1 | 4.514E-2 | 7.814E+2 |
| 4.332E-2 | 8.006E+0 | 4.808E+1 | 5.067E-2 | 5.102E+0 | 6.480E+1 | 1.920E-1 | 3.691E-2 | 7.321E+2 |
| 4.874E-2 | 6.727E+0 | 4.697E+1 | 5.700E-2 | 4.201E+0 | 6.346E+1 | 2.160E-1 | 3.073E-2 | 6.950E+2 |
| 5.415E-2 | 5.741E+0 | 4.595E+1 | 6.333E-2 | 3.520E+0 | 6.234E+1 | 2.400E-1 | 2.596E-2 | 6.666E+2 |
| 6.092E-2 | 4.794E+0 | 4.479E+1 | 7.125E-2 | 2.877E+0 | 6.119E+1 | 2.700E-1 | 2.139E-2 | 6.397E+2 |
| 6.769E-2 | 4.070E+0 | 4.376E+1 | 7.917E-2 | 2.396E+0 | 6.024E+1 | 3.000E-1 | 1.790E-2 | 6.194E+2 |
| 7.446E-2 | 3.501E+0 | 4.286E+1 | 8.708E-2 | 2.026E+0 | 5.944E+1 | 3.300E-1 | 1.518E-2 | 6.037E+2 |
| 8.123E-2 | 3.046E+0 | 4.206E+1 | 9.500E-2 | 1.735E+0 | 5.876E+1 | 3.600E-1 | 1.303E-2 | 5.912E+2 |

whose choice constitutes the hard core of the practical difficulties. A simple power series expansion is not very good for this problem. There are indications, from current work at the University of Illinois, that other choices can improve the convergence considerably. This seems to be the real difficulty with variational calculations at the present time.

ACKNOWLEDGMENTS

This work was motivated by the experimental research led by Frederick C. Brown. To him, and to Leo P. Kadanoff, I am indebted for many stimulating discussions. I am also grateful to S. Kahne and B. Elliot for their invaluable help in the digital computer calculations.